ESC HEART FAILURE
ESC Heart Failure 2024; **11**: 1612–1624
Published online 23 February 2024 in Wiley Online Library (wileyonlinelibrary.com) **DOI:** 10.1002/ehf2.14710

ORIGINAL ARTICLE

A new staging system using right atrial strain in patients with immunoglobulin light-chain cardiac amyloidosis

Hiroki Usuku[1,2,3], Eiichiro Yamamoto[2,3]*, Daisuke Sueta[2,3], Rumi Shinriki[1], Fumi Oike[2,3], Noriaki Tabata[2,3], Masanobu Ishii[2,3], Shinsuke Hanatani[2,3], Tadashi Hoshiyama[2,3], Hisanori Kanazawa[2,3], Yuichiro Arima[2,3], Seiji Takashio[2,3], Yawara Kawano[4], Seitaro Oda[5], Hiroaki Kawano[2,3], Mitsuharu Ueda[3,6] and Kenichi Tsujita[2,3]

[1]*Department of Laboratory Medicine, Kumamoto University Hospital, Kumamoto, Japan;* [2]*Department of Cardiovascular Medicine, Graduate School of Medical Sciences, Kumamoto University, Kumamoto, Japan;* [3]*Center of Metabolic Regulation of Healthy Aging, Kumamoto University Faculty of Life Sciences, Kumamoto, Japan;* [4]*Department of Hematology, Rheumatology, and Infectious Diseases, Graduate School of Medical Science, Kumamoto University, Kumamoto, Japan;* [5]*Department of Diagnostic Radiology, Faculty of Life Sciences, Kumamoto University, Kumamoto, Japan; and* [6]*Department of Neurology, Graduate School of Medical Sciences, Kumamoto University, Kumamoto, Japan*

Abstract

Aims There are minimal data on the prognostic impact of right atrial strain during the reservoir phase (RASr) in patients with immunoglobulin light-chain (AL) cardiac amyloidosis.

Methods and results Among 78 patients who were diagnosed with AL cardiac amyloidosis at Kumamoto University Hospital from 2007 to 2022, 72 patients with sufficient two-dimensional speckle tracking imaging data without chemotherapy before the diagnosis were retrospectively analysed. During a median follow-up of 403 days, 31 deaths occurred. Age and the rate of male sex were not significantly different between the all-cause death group and the survival group (age, 70.4 ± 8.8 years vs. 67.0 ± 10.0 years, $P = 0.14$, male sex, 65% vs. 66%, $P = 0.91$). The estimated glomerular filtration rate (eGFR) was significantly lower, and B-type natriuretic peptide (BNP) and high sensitivity cardiac troponin T (hs-cTnT) were significantly higher, in the all-cause death group versus the survival group (eGFR, 48.2 ± 21.0 mL/min/1.73 m^2 vs. 59.4 ± 24.4 mL/min/1.73 m^2, $P < 0.05$, BNP, 725 [360–1312] pg/mL vs. 123 [81–310] pg/mL, $P < 0.01$, hs-cTnT, 0.12 [0.07–0.18] ng/mL vs. 0.05 [0.03–0.08] ng/mL, $P < 0.01$). Left ventricular (LV) global longitudinal strain (GLS) (LV-GLS), left atrial strain during the reservoir phase (LASr), right ventricular GLS (RV-GLS), and RASr were significantly lower in the all-cause death group versus the survival group (LV-GLS, 8.5 ± 4.3% vs. 11.8 ± 3.8%, $P < 0.01$, LASr, 8.8 ± 7.1% vs. 14.3 ± 8.1%, $P < 0.01$, RV-GLS, 11.6 ± 5.1% vs. 16.4 ± 3.9%, $P < 0.01$, RASr, 10.2 ± 7.3% vs. 20.7 ± 9.5%, $P < 0.01$). RASr was significantly associated with all-cause death after adjusting for RV-GLS, LV-GLS and LASr (hazard ratio [HR]: 0.91, 95% confidence interval [95% CI]: 0.83–0.99, $P < 0.05$). RASr and log-transformed BNP were significantly associated with all-cause death after adjusting for log-transformed troponin T and eGFR (RASr, HR: 0.93, 95% CI: 0.87–1.00, $P < 0.05$; log-transformed BNP, HR: 2.10, 95% CI: 1.17–3.79, $P < 0.05$). The optimal cut-off values were RASr: 16.4% (sensitivity: 66%, specificity: 84%, area under curve [AUC]: 0.81) and BNP: 311.2 pg/mL (sensitivity: 83%, specificity: 78%, AUC: 0.82) to predict all-cause mortality using ROC analysis. Kaplan–Meier analysis revealed that patients with low RASr (<16.4%) or high BNP (>311.2 pg/mL) had a significantly high probability of all-cause death (both, $P < 0.01$). We devised a new staging score by adding 1 point if RASr decreased or BNP levels increased more than each cut-off value. The HR for all-cause death using score 0 as a reference was 5.95 (95% CI: 1.19–29.79; $P < 0.05$) for score 1 and 23.29 (95% CI: 5.37–100.98; $P < 0.01$) for score 2.

Conclusions The new staging system using RASr and BNP predicted prognosis in patients with AL cardiac amyloidosis.

Keywords B-type natriuretic peptide; Immunoglobulin light-chain cardiac amyloidosis; Right atrial strain during the reservoir phase

Received: 16 July 2023; Revised: 9 January 2024; Accepted: 21 January 2024
**Correspondence to: Eiichiro Yamamoto, Department of Cardiovascular Medicine, Graduate School of Medical Sciences, Kumamoto University, 1-1-1 Honjo, Chuo-ku, Kumamoto 860-8556, Japan. Email: eyamamo@kumamoto-u.ac.jp*

Introduction

Immunoglobulin light-chain (AL) amyloidosis is a multisystem disease caused by the deposition of amyloid fibrils in organ tissues, and it arises from misfolded light chains most commonly produced by clonal expansion of monoclonal plasma cells.[1] Cardiac involvement has been noted in approximately 70% of patients with AL amyloidosis[2,3] and is the primary driver of death in these patients.[4]

Myocardial amyloid deposition in cardiac tissues causes dysfunction through both architectural damages and direct myocardial toxicity and oxidative damage by amyloidogenic light chains.[5] Survival staging using B-type natriuretic peptide (BNP) and cardiac troponin can predict a poor prognosis in AL amyloidosis.[6] Echocardiographic findings also provide diagnostic and prognostic information in patients with AL amyloidosis suspected of having cardiac involvement.[7,8] Two-dimensional strain analysis based on speckle-tracking echocardiography has recently been used to detect myocardial deformation. Global reduction of left ventricular (LV) global longitudinal strain (GLS) (LV-GLS) is a significant prognostic factor in cardiac amyloidosis.[9,10] Because cardiac amyloidosis is a diffuse disease that affects all four chambers,[11] we previously revealed the usefulness of left atrial longitudinal strain (LALS) and right ventricular (RV) GLS (RV-GLS) to predict cardiovascular events in wild-type transthyretin amyloid cardiomyopathy (ATTRwt-CM).[12,13] However, the usefulness of right atrial (RA) LS as a predictive factor in patients with AL cardiac amyloidosis has not been sufficiently clarified. Therefore, we investigated whether RALS estimated by two-dimensional speckle-tracking echocardiography provides prognostic information in patients with AL cardiac amyloidosis. We also evaluated a new staging system using biomarkers and echocardiographic findings to predict the prognosis of AL cardiac amyloidosis.

Methods

Study population

Seventy-eight patients were diagnosed with AL cardiac amyloidosis at Kumamoto University Hospital from January 2007 to December 2022. Of these patients, five were excluded because they had no transthoracic echocardiography data at diagnosis or had insufficient two-dimensional speckle-tracking echocardiography data. An additional patient was excluded because he received chemotherapy before the diagnosis of cardiac amyloidosis. The remaining 72 patients diagnosed with AL cardiac amyloidosis were enrolled in this study (*Figure 1*). Baseline clinical characteristics and echocardiographic data at diagnosis were obtained while the patients were clinically stable.

This study conformed to the principles outlined in the Declaration of Helsinki and was approved by the institutional review board and ethics committee of Kumamoto University (No. 1588). The requirement to obtain informed consent was waived because of the low-risk nature of this retrospective study regarding patient identification, and the inability to obtain consent directly from all patients because many patients were already dead. Instead, we announced this study protocol extensively at Kumamoto University Hospital and on our website (http://www2.kuh.kumamoto-u.ac.jp/tyuokensabu/index.html) and gave patients the opportunity to withdraw from the study.

Diagnosis of immunoglobulin light-chain cardiac amyloidosis

The diagnosis of amyloid deposition was based on Congo red staining and apple-green birefringence visualized with

Figure 1 Study flow chart detailing the inclusion and exclusion criteria for the study patients. AL cardiac amyloidosis, immunoglobulin light-chain cardiac amyloidosis; TTE, transthoracic echocardiography.

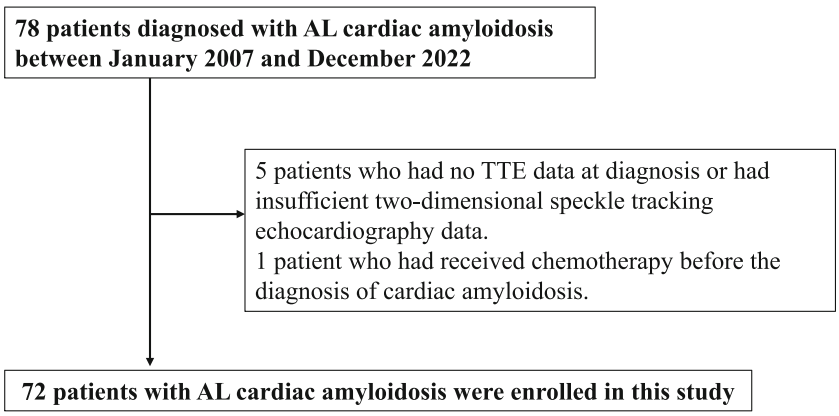

cross-polarized light microscopy in biopsied tissue samples. AL amyloidosis was diagnosed on the basis of positive staining for immunoglobulin light chains by immunohistochemical staining. We diagnosed cardiac amyloidosis when amyloid deposition was observed in the myocardium and typical findings were observed on cardiac magnetic resonance imaging (e.g. LV subendocardial late gadolinium enhancement or significantly elevated native T1 and extracellular volume fraction values). AL cardiac amyloidosis was also diagnosed by echocardiography when a thickened LV wall (interventricular septal thickness at end-diastole (IVSTd) $>$ 12 mm) and +1 or 2 characteristic echo findings (grade $\geq$2 diastolic dysfunction; reduced S', e' and a' velocities ($<$5 cm/s); decreased GLS to $\geq -15\%$) or ECHO score $\geq$ 8 was observed in accordance with 2022 European Society of Cardiology cardio-oncology guidelines.[14]

Previous survival staging system

In accordance with the survival staging system of Lilleness et al.,[6] which uses BNP and cardiac troponin concentrations, we separated the enrolled patients into four groups (stage I, II, IIIa, and IIIb) using the following reported cut-off definitions: stage I, both BNP and high-sensitivity cardiac troponin T (hs-cTnT) lower than the cutoff points (BNP: 81 pg/mL, hs-cTnT: 0.035 ng/mL); stage II: either BNP or hs-cTnT higher than the cutoff point (BNP: 81 pg/mL, hs-cTnT: 0.035 ng/mL); and stage III: both BNP and hs-cTnT higher than the cutoff points (BNP: 81 pg/mL, hs-cTnT: 0.035 ng/mL). Patients in stage III were further divided on the basis of the BNP levels as stage IIIa (BNP $\leq$ 700 pg/mL) and stage IIIb (BNP $>$ 700 pg/mL).

Conventional echocardiographic measurements

Transthoracic echocardiography was performed in patients in a stable condition using the Vivid E95 or 7 (GE Vingmed Ultrasound AS, Horten, Norway), Aplio 500 (Canon Medical Systems Corp., Otawara, Tochigi, Japan), and Epiq 7G (Philips Healthcare, Bothell, WA, USA), which were equipped with a 2.5-MHz phased-array transducer. Conventional echocardiography was performed in accordance with the recommendations of the American Society of Echocardiography (ASE) and the European Association of Cardiovascular Imaging.[15,16] LV wall thickness was acquired in the parasternal long-axis view. LV ejection fraction (LVEF) and LA volume index were calculated using a modified Simpson's method. Peak early diastolic velocity of LV inflow (E velocity), late atrial diastolic velocity of LV inflow (A velocity), and peak early diastolic velocity on the septal corner of the mitral annulus (e') were measured in the apical four-chamber view. Moderate or severe valvular disease in accordance with the ASE guideline[17] was defined as valvular disease in this study. To minimize bias, the echocardiography reviewers were blinded to the patients' clinical history and data.

Two-dimensional speckle-tracking echocardiography

Two-dimensional speckle-tracking echocardiography was performed by one operator (first operator) who was blinded to the clinical data and who differed from the operator who performed the conventional echocardiography. Two-dimensional speckle-tracking echocardiography was performed using cardiac performance analysis with a manual vendor-independent measurement package (TomTec-Arena; TomTec Imaging Systems, Unterschleissheim, Germany). To assess LV strain, the LS, calculated from the echocardiographic images in the four-, three-, and two-chamber views, was determined in 16 segments of the LV in accordance with the ASE guidelines.[15] LV-GLS was calculated as the average LS of these 16 segments. To assess RV-GLS, we evaluated the average value of the longitudinal peak systolic strain from the free wall and the septal wall of the RV in the RV-focused apical four-chamber view.[18] To assess LALS, the regional strain was determined in three segments (septal, roof, and lateral) obtained from echocardiographic images in the four-chamber apical view in accordance with our previous report.[13,19] To assess RALS, the regional strain was determined in three segments (septal, roof, and lateral) obtained from echocardiographic images in the RV-focused apical four-chamber view (*Figure 2*). To evaluate LA and RA strain components, the zero-strain reference was defined at end-diastole. In the present study, we used LA strain during the reservoir phase (LASr) and right atrial strain during the reservoir phase (RASr) as indicators of LA and RA function, respectively, because we previously revealed the prognostic utility of LA reservoir function in cardiac amyloidosis.[13] Strains are described as absolute values. Intraobserver variability was assessed as follows: the first operator re-evaluated RASr measurements from 20 patients 1 month after the initial calculation. Interobserver variability was assessed as follows: the RASr measurements from 20 patients were paired with the measurements of another operator (second operator). The intraobserver and interobserver variabilities were assessed using the intraclass correlation coefficient (ICC). Analysis of the intraobserver and interobserver variabilities showed good correlations for RASr measurements [mean ICC: 0.96, 95% confidence interval (CI): 0.90–0.98, and mean ICC: 0.97, 95% CI: 0.91–0.99, respectively].

Figure 2 Representative example of RA measurement in patients with AL cardiac amyloidosis. White arrow shows RA strain during reservoir phase. RA, right atrial; AL cardiac amyloidosis, immunoglobulin light-chain cardiac amyloidosis.

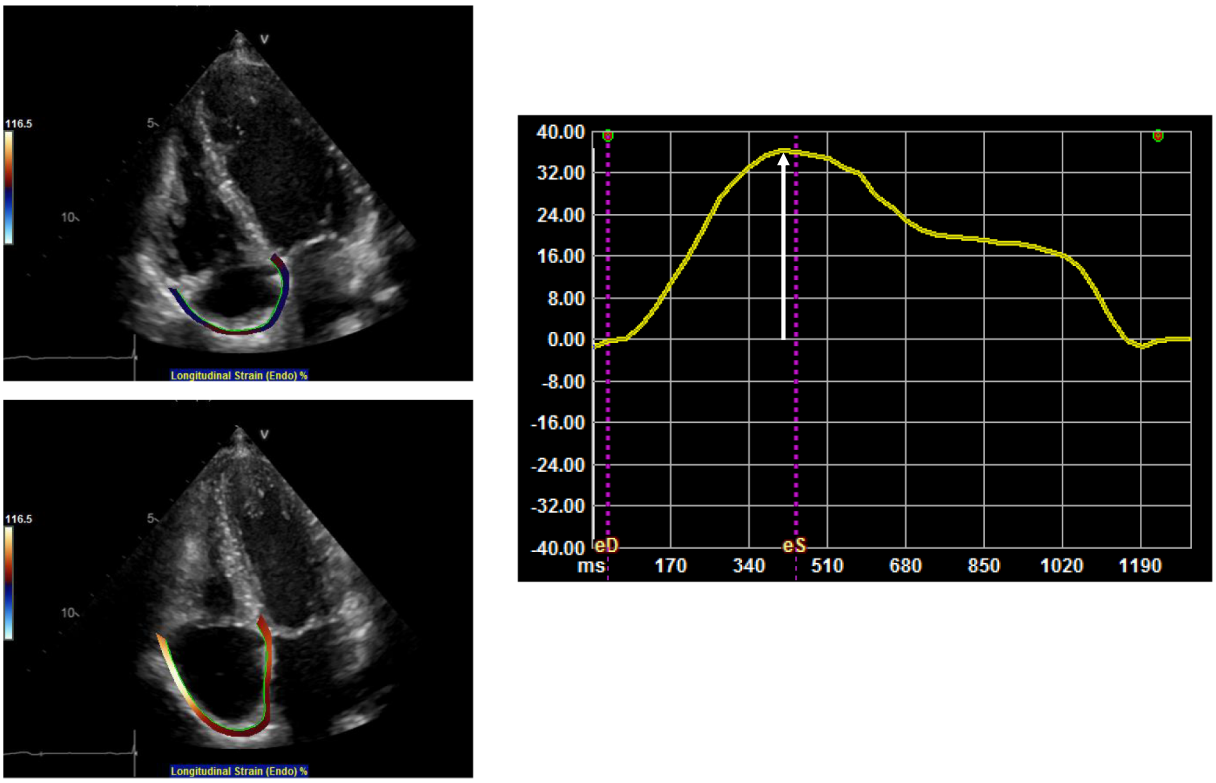

Data collection

For patients who received chemotherapy, laboratory examination and transthoracic echocardiography were performed before starting chemotherapy. Mortality was identified by a search of the patients' medical records and confirmed by a questionnaire and direct contact via a telephone interview with the patient or, if deceased, a family member. These data were confirmed in December 2022.

Statistical analysis

Continuous variables are presented as mean ± standard deviation. Non-normally distributed variables are presented as medians (interquartile range). Categorical variables are presented as frequencies or percentages. The clinical characteristics were compared between the survival group and all-cause death group using Student's *t* test, the Mann–Whitney *U* test, or the chi-squared test. Univariate and multivariate Cox proportional hazard analyses were performed to identify the independent parameters related to all-cause death and to assess the degree of prognostic association. High-sensitivity cardiac troponin T (hs-cTnT) and B-type natriuretic peptide (BNP) concentrations were converted to log-transformed TnT and log-transformed BNP in the Cox proportional hazard analyses. Variables with a *P*-value of <0.05 in the univariate Cox hazard analyses model and which might be clinically important were incorporated in the multivariable Cox hazard analysis. Receiver operating characteristic curves were constructed, and the area under the curve was calculated to assess the ability of RASr and BNP to predict all-cause death and to determine the cutoff values for predicting all-cause death. Kaplan–Meier analysis was used to determine the cumulative incidence of all-cause death, and the log-rank test was used to compare the incidence of all-cause death between the high and low RASr groups, and the BNP groups. Statistical analyses were performed with SPSS for Windows, version 24.0 (IBM Corp., Armonk, NY, USA). A two-tailed *P*-value of <0.05 denoted a statistically significant difference.

Results

Diagnosis of immunoglobulin light-chain cardiac amyloidosis

Among the 72 enrolled patients, 11 patients underwent endomyocardial biopsy, of whom 10 patients had AL amyloid

deposition in the heart. In the other 62 patients, AL amyloid deposition was confirmed in other tissues (skin or abdominal fat pad, *n* = 24, gastrointestinal tract, *n* = 29, kidney, *n* = 9, other tissues, *n* = 4). Cardiac amyloidosis was defined based on amyloid deposition in the myocardium (*n* = 10) or with typical findings on cardiac magnetic resonance imaging (*n* = 36) or echocardiography (IVSTd > 12 mm) (*n* = 26).

Comparison of clinical characteristics between the all-cause death and survival groups

During a median follow-up of 403 days (interquartile range, 146–1195 days), 31 deaths occurred (heart failure, *n* = 16; out-of-hospital sudden death, *n* = 3; ventricular arrhythmia, *n* = 2; infection, *n* = 2; renal failure, *n* = 2; general weakness, *n* = 2; intestinal perforation, *n* = 1; multiple myeloma, *n* = 1; cerebral infarction, *n* = 1; and unknown cause, *n* = 1). No patients received cardiac transplant. *Table 1* shows the clinical characteristics in the all-cause death group and the survival group. The rate of stage II was significantly lower, and the rate of stage IIIb was significantly higher, in the all-cause death group versus the survival group. The rate of hospitalization for heart failure before diagnosis of AL cardiac amyloidosis was significantly higher in the all-cause death group versus the survival group. The rate of New York Heart Association (NYHA) class I and II were significantly lower, and NYHA class III and IV were significantly higher in the all-cause death group vs. the survival group. Among the laboratory findings, the estimated glomerular filtration rate was significantly lower, and BNP and hs-cTnT were significantly higher, in the all-cause death group versus the survival group. Among the conventional echocardiographic findings, LVEF, RV fractional area change (RVFAC), and tricuspid annular plane systolic excursion (TAPSE) were significantly lower, and the LA volume index, IVSTd, E/e' ratio, and the rate of mitral regurgitation were significantly higher in the all-cause death group versus the survival group. Among the two-dimensional speckle-tracking echocardiographic findings, LV-GLS, LASr, RV-GLS, and RASr were significantly lower in the all-cause death group versus the survival group. Regarding cardiac and haematological treatments, the rates of bortezomib and daratumumab administration were significantly lower in the all-cause death group versus the survival group.

Cox proportional hazard analysis for all-cause death

As shown in *Table 2a*, the univariate Cox proportional hazard analysis showed that 20 variables were significantly associated with higher/lower mortality: log-transformed TnT, log-transformed BNP, estimated glomerular filtration rate, stage II, stage IIIb, LAVI, IVSTd, LVEF, E/e' ratio, RVFAC, TAPSE, mitral regurgitation, tricuspid regurgitation, LV-GLS, LASr, RV-GLS, RASr, beta-blocker use, bortezomib use, and daratumumab use. Considering the internal correlation and the number of patients in our study, we created five models to perform multivariate Cox proportional hazard analysis (*Table 2b*). RASr was significantly and independently associated with all-cause death after adjusting for RVFAC, TAPSE, and RV-GLS (Model 1), RV-GLS, LV-GLS and LASr (Model 2), conventional echocardiographic findings (Model 3), conventional prognostic risk factors (Model 4), and medications (Model 5).

Correlation between right atrial strain during the reservoir phase and the other echocardiographic findings

Table 3 shows the correlation between RASr and echocardiographic findings in patients with AL cardiac amyloidosis. Various echocardiographic findings were significantly correlated with RASr. In particular, LV-GLS, LASr, and RV-GLS were significantly correlated with RASr (LV-GLS, $r = 0.71$, $P < 0.01$; LASr, $r = 0.64$, $P < 0.01$; RV-GLS, $r = 0.82$, $P < 0.01$).

Receiver operating characteristic curve analysis for all-cause death

Receiver operating characteristic curve analysis was performed to determine the optimal RASr and BNP cutoff values for predicting all-cause death in patients with AL cardiac amyloidosis. As shown in *Figure 3A*, the area under the curve for RASr for all-cause death was 0.81, and the best cutoff value for RASr was 16.4% (sensitivity, 66%; specificity, 84%). In contrast, the area under the curve for BNP for all-cause death was 0.82 (*Figure 3B*), and the best cutoff value for BNP was 311.2 pg/mL (sensitivity, 83%; specificity, 78%).

Follow-up of patients with high and low right atrial strain during the reservoir phase values or high and low B-type natriuretic peptide values

We divided the patients into two groups using the best cutoff value for RASr into a high RASr group (≥16.4%, *n* = 32) and low RASr group (<16.4%, *n* = 40). Kaplan–Meier analysis demonstrated a significantly higher risk of all-cause death in patients with low versus high RASr ($P < 0.01$, log-rank test) (*Figure 4A*). We also divided the patients into two groups using the best cutoff value for BNP into a high BNP group (≥311.2 pg/mL, *n* = 33) and low BNP group (<311.2 pg/mL, *n* = 36). Kaplan–Meier analysis demonstrated a significantly higher risk of all-cause death in patients with high versus low BNP ($P < 0.01$, log-rank test) (*Figure 4B*).

Table 1 Clinical characteristics between all-cause death group and event-free group

	Event-free group (n = 41)	All-cause death group (n = 31)	P-value
Baseline clinical characteristics			
Age, years	67.0 ± 10.0	70.4 ± 8.8	0.14
Male sex, n (%)	27 (66)	20 (65)	0.91
Body mass index, kg/m^2	22.2 ± 4.3	21.5 ± 3.2	0.48
Past medical history			
Hypertension, n (%)	18 (44)	7 (23)	0.06
Diabetes mellitus, n (%)	6 (15)	2 (6)	0.27
Dyslipidaemia, n (%)	9 (22)	5 (16)	0.54
Current smoking, n (%)	2 (5)	1 (3)	0.75
Arial fibrillation, n (%)	5 (12)	6 (19)	0.40
ICD, n (%)	3 (7)	3 (10)	0.72
Pacemaker, n (%)	4 (10)	5 (16)	0.42
Stage I, n (%)	4/37 (11)	3/28 (11)	0.99
Stage II, n (%)	11/37 (30)	2/28 (7)	<0.05
Stage IIIa, n (%)	20/37 (54)	9/28 (32)	0.08
Stage IIIb, n (%)	2/37 (5)	14/28 (50)	<0.01
Systolic blood pressure, mmHg	115.3 ± 16.6	101.7 ± 15.3	<0.01
Diastolic blood pressure, mmHg	66.8 ± 11.6	63.0 ± 11.2	0.18
Hospitalization for heart failure, n (%)	13 (32)	18 (58)	<0.05
NYHA class 1, n (%)	19 (46)	4 (13)	<0.01
NYHA class II, n (%)	14 (34)	3 (10)	<0.05
NYHA class III, n (%)	8 (20)	16 (52)	<0.01
NYHA class IV, n (%)	0 (0)	8 (26)	<0.01
Laboratory findings			
Haemoglobin level, g/dL	12.7 ± 2.4	12.1 ± 2.0	0.27
eGFR, mL/min/1.73 m^2	59.4 ± 24.4	48.2 ± 21.0	<0.05
BNP, pg/mL	123 [81–310] (n = 41)	725 [360–1312] (n = 30)	<0.01
Hs-cTnT, ng/mL	0.05 [0.03–0.08] (n = 37)	0.12 [0.07–0.18] (n = 29)	<0.01
C-reactive protein, mg/L	0.13 [0.05–0.29]	0.21 [0.05–0.65]	0.39
Difference FLC	257 [72–716] (n = 39)	403 [183–1105] (n = 18)	0.20
Conventional echocardiographic findings			
LAVI, mL/m^2	46.7 ± 21.5	59.2 ± 22.7	<0.05
IVSTd, mm	13.0 ± 2.1	14.3 ± 2.8	<0.05
LVPWTd, mm	12.8 ± 2.1	13.8 ± 2.1	0.06
LVEF, %	60.6 ± 7.6	53.6 ± 9.9	<0.01
E/A	1.36 ± 1.17 (n = 37)	1.92 ± 1.36 (n = 25)	0.09
E/e' ratio	18.2 ± 7.4	24.6 ± 10.8	<0.01
RVFAC, %	29.4 ± 7.4	21.0 ± 8.8	<0.01
TAPSE, mm	18.0 ± 5.1	13.7 ± 4.7	<0.01
RA area, cm^2	16.4 ± 5.5	18.6 ± 5.4	0.10
AS (%)	1 (2)	0 (0)	0.38
MS (%)	0 (0)	1 (3)	0.25
MR (%)	1 (2)	8 (26)	<0.01
TR (%)	1 (2)	4 (13)	0.08
Two-dimensional speckle tracking echocardiographic findings			
LV-GLS, %	11.8 ± 3.8	8.5 ± 4.3	<0.01
LASr, %	14.3 ± 8.1	8.8 ± 7.1	<0.01
RV-GLS, %	16.4 ± 3.9	11.6 ± 5.1	<0.01
RASr, %	20.7 ± 9.5	10.2 ± 7.3	<0.01
Cardiac treatment			
RAS inhibitor, n (%)	9 (22)	11 (35)	0.20
Beta-blocker, n (%)	5 (12)	8 (26)	0.14
Diuretic, n (%)	24 (59)	24 (77)	0.09
Haematological treatment			
Bortezomib, n (%)	17 (41)	6 (19)	<0.05
Daratumumab, n (%)	32 (78)	6 (19)	<0.01

P-values were obtained by Student's t-test, Mann–Whitney U test or chi-squared test.

AS, aortic stenosis; BNP, B-type natriuretic peptide; eGFR, estimated glomerular filtration rate; FLC, free light chain; GLS, global longitudinal strain; hs-cTnT, high sensitivity cardiac troponin T; ICD, implantable cardioverter defibrillator; IVSTd, interventricular septal thickness in diastole; LASr, left atrial strain during reservoir phase; LAVI, left atrial volume index; LV, left ventricle; LVEF, left ventricular ejection fraction; LVPWTd, left ventricular posterior wall thickness in diastole; MR, mitral regurgitation; MS, mitral stenosis; NYHA, New York Heart Association; RA, right atrium; RAS, renin angiotensin system; RASr, right atrium strain during reservoir phase; RV, right ventricle; RVFAC, right ventricular fractional area change; TAPSE, tricuspid annular plane systolic excursion; TR, tricuspid regurgitation.

Table 2a Univariate cox proportional hazards model for all-cause death

	Univariate analysis	
	HR (95% CI)	*P*-value
Age per 1 year	1.04 (1.00–1.08)	0.06
Male sex/yes	0.98 (0.46–2.06)	0.95
Body mass index per 1 kg/m^2	0.96 (0.88–1.05)	0.39
Hypertension/yes	0.48 (0.21–1.12)	0.09
Diabetes mellitus/yes	0.43 (0.10–1.83)	0.26
Dyslipidaemia/yes	0.67 (0.26–1.75)	0.41
Atrial fibrillation/yes	1.83 (0.74–4.51)	0.19
Current smoking/yes	0.71 (0.10–5.25)	0.74
Haemoglobin level per 1 g/dL	0.92 (0.79–1.08)	0.31
Ln TnT per 1	2.12 (1.42–3.15)	<0.01
Ln BNP per 1	3.19 (2.07–4.92)	<0.01
eGFR per 1 mL/min/1.73 m^2	0.98 (0.97–1.00)	<0.05
Difference FLC per 1	1.00 (1.00–1.00)	0.63
Stage I/yes	0.79 (0.24–2.63)	0.70
Stage II/yes	0.22 (0.05–0.93)	<0.05
Stage IIIa/yes	2.96 (1.12–7.80)	0.07
Stage IIIb/yes	9.58 (4.29–21.37)	<0.01
LAVI per 1 mL/m^2	1.02 (1.00–1.04)	<0.05
IVSTd per 1 mm	1.20 (1.04–1.38)	<0.05
LVPWTd per 1 mm	1.15 (0.99–1.34)	0.08
LVEF per 1%	0.94 (0.91–0.97)	<0.01
E/e′ ratio per 1	1.05 (1.02–1.09)	<0.01
RVFAC per 1%	0.91 (0.87–0.95)	<0.01
TAPSE per 1 mm	0.86 (0.80–0.93)	<0.01
RA area per 1 cm^2	1.04 (0.99–1.10)	0.15
Mitral regurgitation/yes	5.67 (2.36–13.63)	<0.01
Tricuspid regurgitation/yes	4.42 (1.51–12.96)	<0.01
LV-GLS per 1%	0.82 (0.74–0.91)	<0.01
LASr per 1%	0.91 (0.85–0.97)	<0.01
RV-GLS per 1%	0.82 (0.76–0.89)	<0.01
RASr per 1%	0.87 (0.83–0.92)	<0.01
RAS inhibitor/yes	1.62 (0.77–3.42)	0.20
Beta-blocker/yes	2.42 (1.07–5.51)	<0.05
Diuretics/yes	2.13 (0.87–5.22)	0.10
Bortezomib/yes	0.36 (0.14–0.90)	<0.05
Daratumumab/yes	0.11 (0.42–0.26)	<0.01

P-value was obtained by the univariate Cox hazard analyses model. BNP, B-type natriuretic peptide; eGFR, estimated glomerular filtration rate; FLC, free light chain; GLS, global longitudinal strain; IVSTd, interventricular septal thickness in diastole; LASr, left atrial strain during reservoir phase; LAVI, left atrial volume index; Ln, natural logarithm; LV, left ventricle; LVEF, left ventricular ejection fraction; LVPWTd, left ventricular posterior wall thickness in diastole; RA, right atrium; RAS, renin angiotensin system; RASr, right atrium strain during reservoir phase; RV, right ventricle; RVFAC, right ventricular fractional area change; TAPSE, tricuspid annular plane systolic excursion; TnT, troponin T.

Next, we divided the patients into four groups using Lilleness et al.'s survival staging system, as follows: survival stage I, II, IIIa, and IIIb. The hazard ratio of all-cause death using stage I as a reference was 5.31 (95% CI: 1.45–19.45, $P < 0.05$) for stage IIIb, but 0.78 (95% CI; 0.21–2.93, $P = 0.71$) for stage IIIa and 0.36 (95% CI: 0.06–2.16, $P = 0.26$) for stage II (*Table 4*). Kaplan–Meier analysis demonstrated no significant difference in all-cause death rates between stage I, stage II, and stage IIIa (*Figure 4C*).

We devised a new survival staging score by adding 1 point if the RASr level decreased or BNP level increased more than the respective cut-off value. The hazard ratio for all-cause mortality, using score 0 as a reference, was 5.95 (95% CI: 1.19–29.79, $P < 0.05$) for score 1 and 23.29 (95% CI: 5.37–100.98, $P < 0.01$) for score 2 (*Table 4*). Kaplan–Meier analysis demonstrated clear differences in all-cause death between score 0, 1 and 2 groups (*Figure 4D*).

Discussion

The present study reported two new findings: (i) RASr by two-dimensional speckle-tracking echocardiography was an important prognostic factor in patients with AL cardiac amyloidosis after adjusting for various factors including RVFAC, TAPSE, LV-GLS, RV-GLS, conventional echocardiographic findings, conventional prognostic risk factors, and medications, and (ii) the new staging system using RASr and BNP was useful to stratify the prognosis in these patients.

Singulane et al. reported that RALS was significantly associated with worse prognosis in AL cardiac amyloidosis.[20] However, the study did not compare RALS with other LS values. Huntjens et al. also revealed the usefulness of RALS to evaluate outcomes in patients with cardiac amyloidosis.[21] However, RA strain did not have greater prognostic power compared with other LS values. The study by Huntjens et al. enrolled patients with various types of amyloid cardiomyopathy. Because the prognosis depends on the type of amyloid cardiomyopathy,[22] specific evaluations should be performed on the basis of each type of amyloid cardiomyopathy. Therefore, in the present study, we enrolled only patients with AL cardiac amyloidosis. To our knowledge, our study is the first to reveal the superiority of RALS over LV-GLS, LALS, and RV-GLS to predict all-cause mortality in these patients.

The normal mechanical function of the RA provides sufficient return of blood to the heart, avoids venous congestion, and protects the upstream organs.[23] The sinoatrial node generates the cardiac impulse, and endocrine function is pivotal in volume regulation in response to acute myocyte stretch and neurohumoral activation.[24] Previous studies showed that RA structural and functional remodelling are prevalent in patients with heart failure (HF), pulmonary arterial hypertension, and hypertrophic cardiomyopathy.[25–27] Furthermore, RA structural and functional remodelling are reported risk predictors in several studies.[28,29]

The RA also plays an important role in modulating the interactions between the performance of the other heart chambers. Therefore, in patients with AL cardiac amyloidosis, the RA is affected by both direct amyloid deposition and the other chambers. The present study revealed that RASr was significantly correlated with RV-GLS and LASr, indicating that RA function was affected by RV function and LA function. Because RV dysfunction can be a late consequence of changes in the pulmonary circulation that result from HF, changes in

Table 2b Multivariate Cox proportional hazards model for all cause death

	Model 1		Model 2		Model 3	
	HR (95% CI)	*P*-value	HR (95% CI)	*P*-value	HR (95% CI)	*P*-value
RVFAC per 1%	0.98 (0.91–1.05)	0.50				
TAPSE per 1 mm	0.96 (0.87–1.05)	0.37				
RV-GLS per 1%	0.98 (0.83–1.16)	0.82	0.94 (0.82–1.09)	0.43		
LV-GLS per 1%			0.96 (0.83–1.12)	0.63		
LASr per 1%			1.00 (0.94–1.06)	0.89		
LAVI per 1 mL/m^2					0.99 (0.97–1.02)	0.54
IVSTd per 1 mm					1.30 (1.01–1.67)	<0.05
LVEF per 1%					1.01 (0.94–1.09)	0.85
E/e′/1					0.97 (0.91–1.04)	0.37
Mitral regurgitation/yes					39.11 (6.91–221.43)	<0.01
Tricuspid regurgitation/yes					7.45 (1.27–43.72)	<0.05
RASr per 1%	0.91 (0.84–0.98)	<0.05	0.91 (0.83–0.99)	<0.05	0.87 (0.80–0.95)	<0.01

	Model 4		Model 5	
	HR (95% CI)	*P*-value	HR (95% CI)	*P*-value
Ln TnT/1	1.22 (0.61–2.47)	0.57		
Ln BNP/1	2.10 (1.17–3.79)	<0.05		
eGFR per 1 mL/min/1.73 m^2	1.00 (0.98–1.02)	0.64		
Beta-blocker/yes			1.62 (0.69–3.79)	0.27
Bortezomib/yes			0.33 (0.12–0.95)	<0.05
Daratumumab/yes			0.12 (0.04–0.31)	<0.01
RASr per 1%	0.93 (0.87–1.00)	<0.05	0.90 (0.85–0.94)	<0.01

P-value was obtained by the multivariate Cox hazard analysis.
eGFR, estimated glomerular filtration rate; GLS, global longitudinal strain; IVSTd, interventricular septal thickness in diastole; LASr, left atrial strain during reservoir phase; LAVI, left atrial volume index; Ln, natural logarithm; LV, left ventricle; LVEF, left ventricular ejection fraction; RASr, right atrium strain during reservoir phase; RV, right ventricle; RVFAC, right ventricular fractional area change; TAPSE, tricuspid annular plane systolic excursion; TnT, troponin T; BNP, B-type natriuretic peptide.

Table 3 Correlation between RASr and the other echocardiographic findings

Variables	*R*	*P*-value
LAVI per 1 mL/m^2	−0.22	0.07
IVSTd per 1 mm	−0.31	<0.01
LVPWTd per 1 mm	−0.38	<0.01
LVEF per 1%	0.51	<0.01
E/A ratio per 1	−0.40	<0.01
E/e′ ratio per 1	−0.45	<0.01
RVFAC per 1%	0.65	<0.01
TAPSE per 1 mm	0.57	<0.01
RA area per 1cm^2	−0.45	<0.01
LV-GLS per 1%	0.71	<0.01
LASr per 1%	0.64	<0.01
RV-GLS per 1%	0.82	<0.01

P-value was obtained by using Pearson's method.
^{99m}Tc-PYP scintigraphy, ^{99m}Tc-pyrophosphate scintigraphy; IVSTd, interventricular septal thickness in diastole; LAVI, left atrial volume index; LVEF, left ventricular ejection fraction; LVPWTd, left ventricular posterior wall thickness in diastole; RVFAC, right ventricular fractional area change; RVFWLS, right ventricular free wall longitudinal strain; RV-GLS, right ventricular global longitudinal strain; TAPSE, tricuspid annular plane systolic excursion.

RA function can aid in the assessment of right heart function. Therefore, RA function is one of the responses to changes in RV compliance and diastolic function early in the course of HF. Additionally, LV dysfunction worsens RV dysfunction because of pulmonary venous hypertension, ventricular interdependence, neurohormonal interactions, and RV myocardial ischemia.[30] LA dysfunction is usually correlated with worse impairment of LV diastolic function because high LV filling pressure leads to deterioration of LA function as a result of hemodynamic overload and mechanical stretching of the LA wall.[31] Therefore, RA function is thought to be affected by direct LA and RV dysfunction and indirect LV dysfunction. In addition, amyloid deposition occurs in all chambers.[11] Because RA is the lowest pressured chamber, the effect of amyloid deposition may be higher in RA than in other chambers. We speculate that RASr could provide greater prognostic power compared with LV-GLS, LASr, and RV-GLS in patients with AL cardiac amyloidosis because RA is the lowest pressured chamber and RA dysfunction might reflect the overall burden of LV, LA, and RV dysfunction, and amyloid deposition.

The RA is now being recognized as more than a passive filling chamber. During the cardiac cycle, the RA serves three primary functions: (i) a reservoir function, (ii) a conduit function, and (iii) a booster pump function.[25] The present study revealed the usefulness of RA reservoir function to evaluate the prognosis in patients with AL cardiac amyloidosis. However, we could not evaluate conduit function and booster pump function because many patients' data did not include booster pump function. It is well known that the rate of atrial fibrillation is high in patients with amyloid cardiomyopathy.[32]

Figure 3 Receiver operator characteristic curve analysis of RASr (A) and BNP (B) for predicting all-cause death. RASr, right atrial strain during the reservoir phase; BNP, B-type natriuretic peptide; AUC, area under the curve.

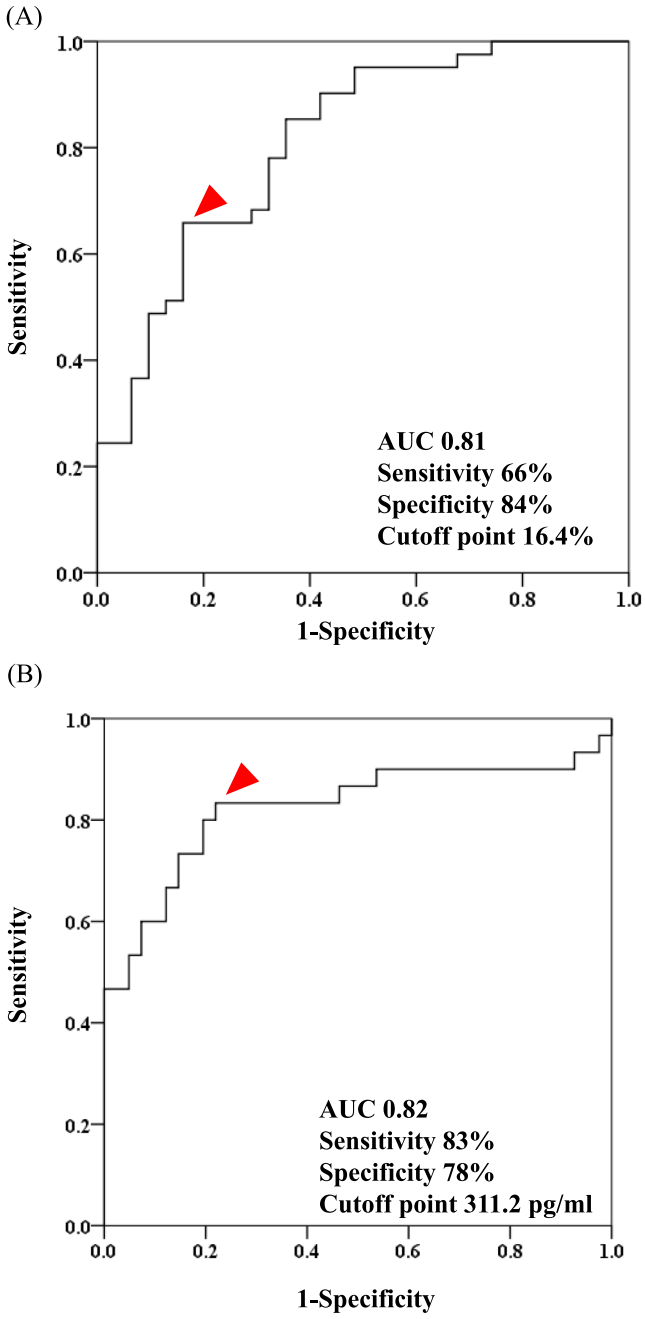

As a result, clinically, there is no booster pump function in many patients with amyloid cardiomyopathy. In our present study, the rate of atrial fibrillation was not different between the all-cause death group and event-free group, indicating the prognostic implications of abnormal RASr is likely independent of atrial fibrillation. Therefore, the use of RASr is clinically relevant as a prognostic factor in patients with AL cardiac amyloidosis in the clinical setting.

A previous survival staging system using BNP and cardiac troponin predicted a poor prognosis in AL cardiac amyloidosis.[6] However, in the present study, there were no significant differences in prognosis between stage I, stage II, and stage IIIa, using the previous system. Our study revealed that hs-cTnT was not significantly useful to predict the prognosis in patients with AL cardiac amyloidosis, which might be the reason why the previous survival staging system was

Figure 4 Kaplan–Meier curves for all-cause death in patients with AL cardiac amyloidosis with high or low RASr (A) and low or high BNP (B) based on a previously reported staging system: stage I, II, IIIa and IIIb (C), and the new staging system: score 0, 1, and 2 (D). AL cardiac amyloidosis, immunoglobulin light-chain cardiac amyloidosis; RASr, right atrial strain during the reservoir phase.

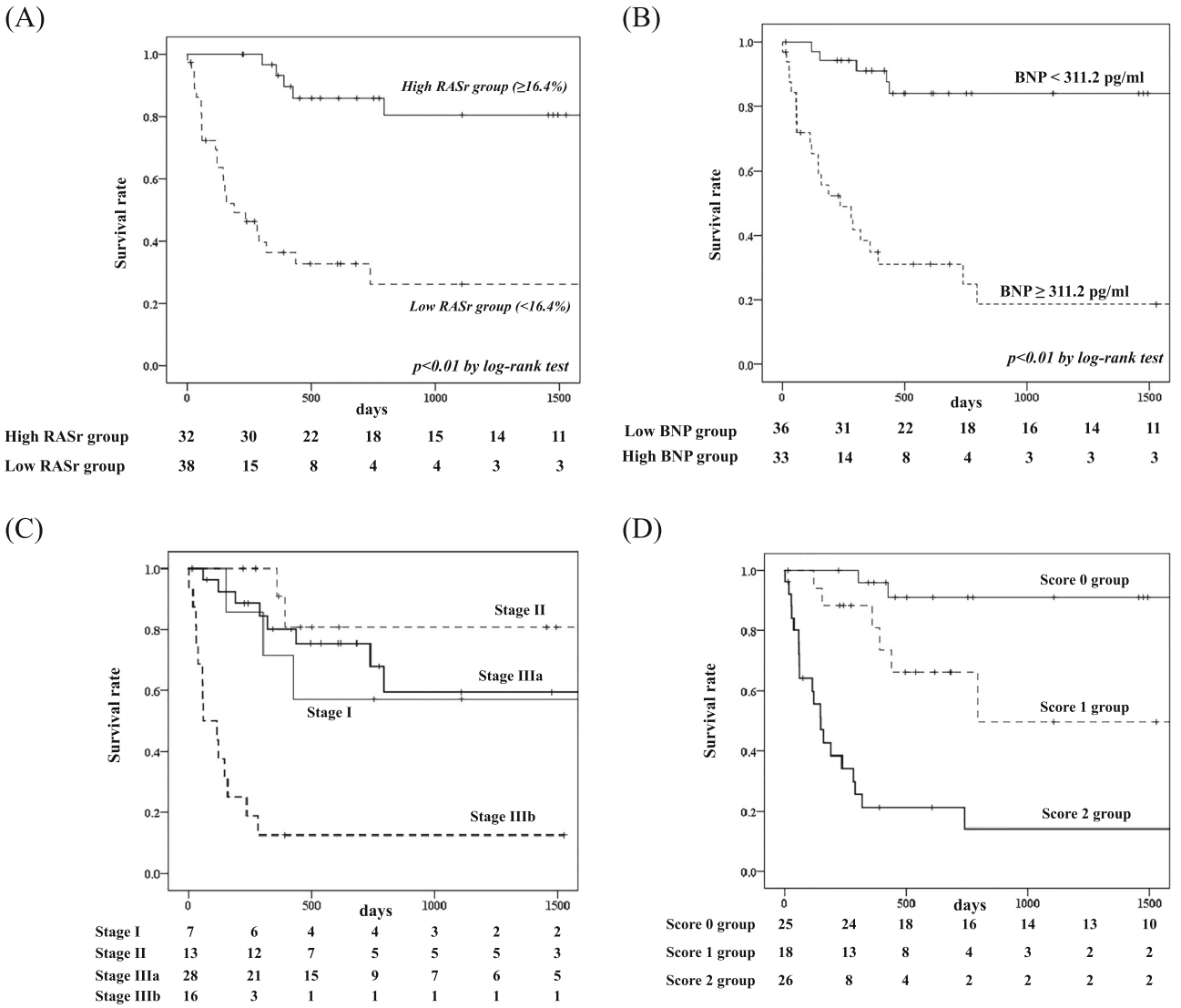

Table 4 Cox proportional hazards model for all cause death by stage and score

Stage	HR (95% CI)	*P*-value	Score	HR (95% CI)	*P*-value
I	Ref.			Ref.	
II	0.36 (0.06–2.16)	0.26	0	5.95 (1.19–27.79)	<0.05
IIIa	0.78 (0.21–2.93)	0.71	1	23.29 (5.37–100.98)	<0.01
IIIb	5.31 (1.45–19.45)	<0.05	2		

P-value was obtained by the Cox hazard analysis model.

not useful in the early stage. In contrast, the new staging system described in this study, which uses RASr and BNP clearly stratified the enrolled patients' prognostic risk into three groups. This was because RASr was significantly and independently associated with prognosis in patients with AL cardiac amyloidosis after adjusting for BNP. Therefore, this new staging system might be useful even in the early stage of AL cardiac amyloidosis to stratify patients' prognosis.

The addition of daratumumab to classical medical therapy was recently shown to be associated with survival free from major organ deterioration or hematologic progression in patients with newly diagnosed AL amyloidosis.[33] Therefore, daratumumab combination therapy represents an important emerging first-line treatment option for patients with systemic AL amyloidosis. However, few data are available regarding prognostic echocardiographic factors in patients with daratumumab therapy. Our study revealed that RALS was independently associated with all-cause mortality even after adjusting for administration of daratumumab therapy. This result indicates that RALS is an important prognostic factor even in patients with daratumumab therapy. Thus, daratumumab therapy should be started in the early stage of AL cardiac amyloidosis, when RA function is fully preserved. Cardiac transplantation is one of the other therapeutic options for severe AL cardiac amyloidosis.[34] In Japan, however, cardiac transplantation is not usually performed in patients with AL cardiac amyloidosis because almost of these patients are high age and their disease progression is generally rapid. Therefore, we could not evaluate the effect of cardiac transplantation on the usefulness of RALS in patients with AL cardiac amyloidosis in our present study.

We previously reported the usefulness of LA and RV strain for prognostic factor in patients with ATTRwt-CM.[12,13] However, we had no data about the usefulness of RALS in these patients. Therefore, we have to evaluate the usefulness of RALS for prognostic factor in patients with ATTR-CM in the future.

Study limitations

This study has several limitations. First, this was a retrospective single-centre study that included a small number of patients with AL cardiac amyloidosis. This was important limitation in our present study. Therefore, further multicentre prospective studies with more patients are needed to validate our results. Second, echocardiographic images were obtained using several different brands of ultrasound machines. We performed the two-dimensional speckle-tracking echocardiography analysis using vendor-independent software (TomTec Image-Arena™). Although significant correlations have been shown in the LS values analysed using vendor-independent software for paired images obtained from different ultrasound machines,[35] inter-machine variability may still have affected our study results. Third, several patients were diagnosed with AL cardiac amyloidosis before the RV-focused apical four-chamber view was recommended. Therefore, we had no choice but to use the apical four-chamber view to evaluate RASr and RV-GLS in these patients. In addition, the e' lateral line was not measured in several patients because the patients were diagnosed with AL cardiac amyloidosis before the e' lateral line was recommended. Therefore, we used only the e' septal line to evaluate LV diastolic function in the present study. Fourth, the rate of stage 3b was 50% in all-cause death group. In contrast, the rate of stage 3b was only 5% in event-free group. In addition, the components of previous survival staging system: BNP and hs-cTnT were significantly associated with all-cause death by univariate Cox proportional hazard model. These results indicated that many patients in all-cause death group was in the advanced stage and those in event-free group were in the early stage, and most of these two populations were not overlapping. In our present study, however, RASr was significantly and independently associated with all-cause death adjusting for BNP and hs-cTnT. Thus, RASr might be a significant and independent prognostic factor after adjusting for previous survival staging system in patients with AL cardiac amyloidosis. Fifth, only 6 patients in the all-cause death group received daratumumab therapy. Thus, the event-free survival group received more treatment than the all-cause death group. This is an important limitation that RASr was a significant prognostic marker independent of daratumumab therapy.

Despite these limitations, the present study demonstrated the importance of RA function estimated by two-dimensional strain analysis compared with LVLS, LALS, and RVLS, and the usefulness of new staging system using BNP and RASr in patients with AL cardiac amyloidosis. We believe that our results have important clinical value.

Conclusions

RASr has prognostic value in patients with AL cardiac amyloidosis and provides greater prognostic power than that of LV-GLS, LASr, and RV-GLS. The new staging system demonstrated by this study, using RASr and BNP, might be useful for predicting prognosis in patients with AL cardiac amyloidosis.

Funding

This study was supported in part by a Grant-in-Aid for Scientific Research (grant number 20K17087) from the Ministry of Education, Culture, Sports, Science and Technology of Japan to DS; a Grant-in-Aid for Scientific Research (grant number 20K08476) from the Japan Society for the Promotion of Science to HU; and a research grant from Pfizer Japan Incorporated to HU.

Acknowledgements

We thank Jane Charbonneau, DVM, from Edanz (https://jp.edanz.com/ac) for editing a draft of this manuscript.

Conflict of interest

None declared.

References

1. Palladini G, Milani P, Merlini G. Management of AL amyloidosis in 2020. *Blood* 2020;**136**:2620-2627. doi:10.1182/hematology.2020006913
2. Kyle RA, Greipp PR, O'Fallon WM. Primary systemic amyloidosis: Multivariate analysis for prognostic factors in 168 cases. *Blood* 1986;**68**:220-224.
3. Milani P, Merlini G, Palladini G. Light chain amyloidosis. *Mediterr J Hematol Infect Dis* 2018;**10**:e2018022. doi:10.4084/MJHID.2018.022
4. Gillmore JD, Wechalekar A, Bird J, Cavenagh J, Hawkins S, Kazmi M, *et al*. Guidelines on the diagnosis and investigation of AL amyloidosis. *Br J Haematol* 2015;**168**:207-218. doi:10.1111/bjh.13156
5. Brenner DA, Jain M, Pimentel DR, Wang B, Connors LH, Skinner M, *et al*. Human amyloidogenic light chains directly impair cardiomyocyte function through an increase in cellular oxidant stress. *Circ Res* 2004;**94**:1008-1010. doi:10.1161/01.RES.0000126569.75419.74
6. Lilleness B, Ruberg FL, Mussinelli R, Doros G, Sanchorawala V. Development and validation of a survival staging system incorporating BNP in patients with light chain amyloidosis. *Blood* 2019;**133**:215-223. doi:10.1182/blood-2018-06-858951
7. Cueto-Garcia L, Reeder GS, Kyle RA, Wood DL, Seward JB, Naessens J, *et al*. Echocardiographic findings in systemic amyloidosis: Spectrum of cardiac involvement and relation to survival. *J Am Coll Cardiol* 1985;**6**:737-743. doi:10.1016/s0735-1097(85)80475-7
8. Kristen AV, Perz JB, Schonland SO, Hegenbart U, Schnabel PA, Kristen JH, *et al*. Non-invasive predictors of survival in cardiac amyloidosis. *Eur J Heart Fail* 2007;**9**:617-624. doi:10.1016/j.ejheart.2007.01.012
9. Quarta CC, Solomon SD, Uraizee I, Kruger J, Longhi S, Ferlito M, *et al*. Left ventricular structure and function in transthyretin-related versus light-chain cardiac amyloidosis. *Circulation* 2014;**129**:1840-1849. doi:10.1161/CIRCULATIONAHA.113.006242
10. Pun SC, Landau HJ, Riedel ER, Jordan J, Yu AF, Hassoun H, *et al*. Prognostic and added value of two-dimensional global longitudinal strain for prediction of survival in patients with light chain amyloidosis undergoing autologous hematopoietic cell transplantation. *J Am Soc Echocardiogr* 2018;**31**:64-70. doi:10.1016/j.echo.2017.08.017
11. Falk RH. Diagnosis and management of the cardiac amyloidoses. *Circulation* 2005;**112**:2047-2060. doi:10.1161/CIRCULATIONAHA.104.489187
12. Usuku H, Takashio S, Yamamoto E, Yamada T, Egashira K, Morioka M, *et al*. Prognostic value of right ventricular global longitudinal strain in transthyretin amyloid cardiomyopathy. *J Cardiol* 2022;**80**:56-63. doi:10.1016/j.jjcc.2022.02.010
13. Oike F, Usuku H, Yamamoto E, Yamada T, Egashira K, Morioka M, *et al*. Prognostic value of left atrial strain in patients with wild-type transthyretin amyloid cardiomyopathy. *ESC Heart Fail* 2021;**8**:5316-5326. doi:10.1002/ehf2.13621
14. Lyon AR, López-Fernández T, Couch LS, Asteggiano R, Aznar MC, Bergler-Klein J, *et al*. 2022 ESC guidelines on cardio-oncology developed in collaboration with the European Hematology Association (EHA), the European Society for Therapeutic Radiology and Oncology (ESTRO) and the international cardio-oncology society (IC-OS). *Eur Heart J* 2022;**43**:4229-4361. doi:10.1093/eurheartj/ehac244
15. Lang RM, Badano LP, Mor-Avi V, Afilalo J, Armstrong A, Ernande L, *et al*. Recommendations for cardiac chamber quantification by echocardiography in adults: An update from the American Society of Echocardiography and the European Association of Cardiovascular Imaging. *J Am Soc Echocardiogr* 2015;**28**:1-39.e14. doi:10.1093/ehjci/jew041
16. Nagueh SF, Smiseth OA, Appleton CP, Byrd BF 3rd, Dokainish H, Edvardsen T, *et al*. Recommendations for the evaluation of left ventricular diastolic function by echocardiography: An update from the American Society of Echocardiography and the European Association of Cardiovascular Imaging. *J Am Soc Echocardiogr* 2016;**29**:277-314. doi:10.1016/j.echo.2016.01.011
17. Zoghbi WA, Adams D, Bonow RO, Enriquez-Sarano M, Foster E, Grayburn PA, *et al*. Recommendations for noninvasive evaluation of native valvular regurgitation: A report from the American Society of Echocardiography developed in collaboration with the Society for Cardiovascular Magnetic Resonance. *J Am Soc Echocardiogr* 2017;**30**:303-371. doi:10.1016/j.echo.2017.01.007
18. Badano LP, Kolias TJ, Muraru D, Abraham TP, Aurigemma G, Edvardsen T, *et al*. Standardization of left atrial, right ventricular, and right atrial deformation imaging using two-dimensional speckle tracking echocardiography: A consensus document of the EACVI/ASE/industry task force to standardize deformation imaging. *Eur Heart J Cardiovasc Imaging* 2018;**19**:591-600. doi:10.1093/ehjci/jey042
19. Oike F, Usuku H, Yamamoto E, Marume K, Takashio S, Ishii M, *et al*. Utility of left atrial and ventricular strain for diagnosis of transthyretin amyloid cardiomyopathy in aortic stenosis. *ESC Heart Fail* 2022;**9**:1976-1986. doi:10.1002/ehf2.13909
20. Singulane CC, Slivnick JA, Addetia K, Asch FM, Sarswat N, Soulat-Dufour L, *et al*. Prevalence of right atrial impairment and association with outcomes in cardiac amyloidosis. *J Am Soc Echocardiogr* 2022;**35**:829-35.e1. doi:10.1016/j.echo.2022.03.022
21. Huntjens PR, Zhang KW, Soyama Y, Karmpalioti M, Lenihan DJ, Gorcsan J 3rd. Prognostic utility of echocardiographic atrial and ventricular strain imaging in patients with cardiac amyloidosis. *JACC Cardiovasc Imaging* 2021;**4**:1508-1519. doi:10.1016/j.jcmg.2021.01.016
22. Ng B, Connors LH, Davidoff R, Skinner M, Falk RH. Senile systemic amyloidosis presenting with heart failure: a comparison with light chain-associated amyloidosis. *Arch Intern Med* 2005;**165**:1425-1429. doi:10.1001/archinte.165.12.1425
23. Gaynor SL, Maniar HS, Prasad SM, Steendijk P, Moon MR. Reservoir and conduit function of right atrium: Impact on right ventricular filling and cardiac output. *Am J Physiol Heart Circ Physiol* 2005;**288**:H2140-H2145. doi:10.1152/ajpheart.00566.2004
24. Goetze JP, Bruneau BG, Ramos HR, Ogawa T, de Bold MK, de Bold AJ. Cardiac natriuretic peptides. *Nat Rev Cardiol* 2020;**17**:698-717. doi:10.1038/s41569-020-0381-0
25. Jain S, Kuriakose D, Edelstein I, Ansari B, Oldland G, Gaddam S, *et al*. Right atrial phasic function in heart failure with preserved and reduced ejection fraction. *JACC Cardiovasc Imaging* 2019;**12**:1460-1470. doi:10.1016/j.jcmg.2018.08.020
26. Jone PN, Schäfer M, Li L, Craft M, Ivy DD, Kutty S. Right atrial deformation in predicting outcomes in pediatric pulmonary hypertension. *Circ Cardiovasc Imaging* 2017;**10**: doi:10.1161/CIRCIMAGING.117.006250

27. Huang J, Yang C, Ni CF, Yan ZN, Fan L, Song XT. Right atrial function assessed by volume-derived values and speckle tracking echocardiography in patients with hypertrophic cardiomyopathy. *BMC Cardiovasc Disord* 2020; **20**:335. doi:10.1186/s12872-020-01610-1
28. Sallach JA, Tang WH, Borowski AG, Tong W, Porter T, Martin MG, *et al*. Right atrial volume index in chronic systolic heart failure and prognosis. *JACC Cardiovasc Imaging* 2009;**2**:527-534. doi:10.1016/j.jcmg.2009.01.012
29. Li Y, Guo J, Li W, Xu Y, Wan K, Xu Z, *et al*. Prognostic value of right atrial strain derived from cardiovascular magnetic resonance in non-ischemic dilated cardiomyopathy. *J Cardiovasc Magn Reson* 2022;**24**:54. doi:10.1186/s12968-022-00894-w
30. Haddad F, Doyle R, Murphy DJ, Hunt SA. Right ventricular function in cardiovascular disease, part II: Pathophysiology, clinical importance, and management of right ventricular failure. *Circulation* 2008;**117**:1717-1731. doi:10.1161/CIRCULATIONAHA.107.653584
31. Guan Z, Zhang D, Huang R, Zhang F, Wang Q, Guo S. Association of left atrial myocardial function with left ventricular diastolic dysfunction in subjects with preserved systolic function: A strain rate imaging study. *Clin Cardiol* 2010;**33**:643-649. doi:10.1002/clc.20784
32. Kitaoka H, Izumi C, Izumiya Y, Inomata T, Ueda M, Kubo T, *et al*. JCS 2020 Guideline on Diagnosis and Treatment of Cardiac Amyloidosis. *Circ J* 2020;**84**:1610-1671. doi:10.1253/circj.CJ-20-0110
33. Kastritis E, Palladini G, Minnema MC, Wechalekar AD, Jaccard A, Lee HC, *et al*. Daratumumab-based treatment for immunoglobulin light-chain amyloidosis. *N Engl J Med* 2021;**385**:46-58. doi:10.1056/NEJMoa2028631
34. Gray Gilstrap L, Niehaus E, Malhotra R, Ton VK, Watts J, Seldin DC, *et al*. Predictors of survival to orthotopic heart transplant in patients with light chain amyloidosis. *J Heart Lung Transplant* 2014;**33**:149-156. doi:10.1016/j.healun.2013.09.004
35. Nagata Y, Takeuchi M, Mizukoshi K, Wu VC, Lin FC, Negishi K, *et al*. Intervendor variability of two-dimensional strain using vendor-specific and vendor-independent software. *J Am Soc Echocardiogr* 2015;**28**:630-641. doi:10.1016/j.echo.2015.01.021